Decay of Flow Birefringence in Dispersions of Charged Colloidal Rods: Effect of Double-Layer Interactions

ARTICLE *in* LANGMUIR · DECEMBER 1997

Impact Factor: 4.46 · DOI: 10.1021/la9708593

3 AUTHORS, INCLUDING:

Albert P Philipse
Utrecht University
189 PUBLICATIONS **6,443** CITATIONS

SEE PROFILE

Decay of Flow Birefringence in Dispersions of Charged Colloidal Rods: Effect of Double-Layer Interactions

Anieke M. Wierenga, Albert P. Philipse,* and Eric M. Reitsma

Van 't Hoff Laboratory for Physical and Colloid Chemistry, Debye Research Institute, Utrecht University, Padualaan 8, 3584 CH Utrecht, The Netherlands

Received August 4, 1997. In Final Form: October 6, 1997[⊗]

The rotational diffusion of charged colloidal boehmite needles in aqueous dispersions was assessed from the decay rate of optical birefringence after cessation of a shear flow. The strong dependence of the characteristic relaxation time τ_r on the ionic strength and the boehmite rod concentration can be described by a rescaling of the particle concentrations in terms of an "effective rotational volume" which takes the electric double layers into account. This dynamic rescaling is obeyed over a wide range of initial shear rates. Rotational relaxation times diverge when the effective particle concentration approaches the threshold density for the formation of a space-filling gel.

1. Introduction

The majority of rodlike colloids (e.g., imogolite,[1] boehmite,[2] TMV,[3] and FD-virus[4]) are charged and surrounded by electric double layers. In experimental and theoretical studies[5−10] of the rotational diffusion of rods, electric double layer effects are usually ignored. It is clear, though, that these interactions will have a significant effect on the rotational diffusion, in particular at low electrolyte concentrations, where surface potentials are only weakly screened. Here we present a study on the effect of double layer interactions on the rotational diffusion of charged colloidal boehmite (AlOOH) rods in aqueous dispersions. These rigid needles are appropriate model colloids for this purpose. They are fairly monodisperse and their dimensions can be controlled in the chemical synthesis.[2] Moreover, the boehmite rods are small enough (typical length 100−200 nm) to exhibit Brownian motion. In addition, the optical transparency of the aqueous boehmite dispersions renders them suitable for (rheo-) optic techniques.

The low-shear rheology of aqueous boehmite dispersions has been studied in detail.[11,12] At low ionic strength, the rheology of the dispersions is largely determined by electric double layer interactions. Above a critical volume fraction, Φ_{gel}, long-range double layer repulsions "freeze" the rods into a space-filling structure. Such a structure, which exhibits a shear yield stress, is called a "repulsive" gel.[12] In dialyzed dispersions of boehmite with aspect ratio $r \approx 22.5$, the critical gel value was found to be as low as $\Phi_{gel} \approx 0.3\%$. For volume fractions $\Phi \geq \Phi_{gel}$, the dispersions exhibit permanent optical birefringence and dynamic light scattering data confirm that Brownian diffusion is arrested.[12] For liquid-like dispersions without yield stress ($\Phi < \Phi_{gel}$), an interesting dynamic rescaling of the particle concentration describes the electrolyte and particle concentration dependence of the low-shear viscosity data.[11] Here we study the rotational dynamics of the rods at concentrations just below the gel density by measuring the relaxation of optical birefringence after cessation of a shear flow. The aim of this paper is to investigate the rotational dynamics on approach of the gel density and to determine whether for this dynamics the same scaling applies as found for the low-shear viscosity.

Before we discuss relaxation curves in sections 4 and 5, we recapitulate the concept of dynamic rescaling in section 2 and describe the dispersions and experimental setup in section 3.

2. Dynamic Rescaling

Rodlike Brownian particles in an initially isotropic dispersion will align in a shear field when the shear rate $\dot{\gamma}$ dominates the rotational diffusion, i.e., when the rotational Péclet number, $Pe_{rot} = \dot{\gamma}/D_r > 1$, with D_r the rotational diffusion coefficient. Due to the induced orientational anisotropy, the sheared sample will exhibit optical birefringence. After cessation of the flow, only Brownian and interparticle forces affect the rods, and the birefringence Δn will decay as[13]

$$\Delta n/\Delta n_{ss} = \exp^{-t/\tau_r} \quad (1)$$

with Δn_{ss} the birefringence during steady shear and $\tau_r = (6D_r)^{-1}$ the rotational relaxation time. At infinite dilution, the rotational diffusion coefficient $D_{r,0}$ for a rod with length L and diameter D is[14−16]

$$D_{r,0} = \frac{3kT}{\pi\eta_0 L^3}(\ln(L/D) - \delta) \quad (2)$$

where kT is the thermal energy, η_0 the solvent viscosity, and δ a constant (for the boehmite rods, $\delta = 0.8$). In nondilute dispersions, rod−rod interactions hinder the rotational motion. As soon as the rod concentration is high enough for rotational volumes ($\sim L^3$) of different rods

* To whom correspondence should be addressed.

[⊗] Abstract published in *Advance ACS Abstracts,* December 1, 1997.

(1) Donkai, N.; Inagaka, H.; Kajiwara, K.; Urakawa, H.; Schmidt, M. *Macromol. Chem.* **1985**, *186*, 2623.
(2) Buining, P. A.; Pathmamanoharan, C.; Jansen, J. B. H.; Lekkerkerker, H. N. W. *J. Am. Ceram. Soc.* **1991**, *74*, 1303.
(3) Lauffer, M. A. *J. Am. Chem. Soc.* **1944**, *66*, 1188.
(4) Graf, C.; Kramer, H.; Deggelman, M.; Hagenbuchle, M.; Johner, C.; Martin, C.; Weber, R. *J. Chem. Phys.* **1993**, *98*, 4920.
(5) Doi, M.; Edwards, S. F. *J. Chem. Soc., Faraday Trans. 2* **1978**, *74*, 560.
(6) Doi, M.; Edwards, S. F. *J. Chem Soc., Faraday Trans. 2* **1978**, *74*, 918.
(7) Edwards, S. F.; Evans, K. E. *J. Chem. Soc., Faraday Trans. 2* **1982**, *78*, 113.
(8) Sato, T.; Teramoto, A. *Macromolecules* **1991**, *24*, 193.
(9) Teraoka, I.; Hayakawa, R. *J. Chem. Phys.* **1989**, *91*, 2643.
(10) Tracy, M. A.; Pecora, R. *Annu. Rev. Phys. Chem.* **1992**, *43*, 525.
(11) Wierenga, A. M.; Philipse, A. P. *Langmuir* **1997**, *13*, 4575.
(12) Wierenga, A. M.; Philipse, A. P.; Lekkerkerker, H. N. W.; Boger, D. V. *Langmuir,* in press.
(13) Doi, M.; Edwards, S. F. *The Theory of Polymer Dynamics*; Clarendon Press: Oxford, 1988.
(14) Broersma, S. *J. Chem. Phys.* **1960**, *32*, 1632.
(15) Broersma, S. *J. Chem. Phys.* **1981**, *74*, 6989.
(16) Tirado, M. M.; Garcia de la Torre, J. *J. Chem Phys.* **1980**, *73*, 1986.

S0743-7463(97)00859-7 CCC: $14.00

to continuously overlap, the rods become "entangled" and the rotational motion of the rods is severely restricted. The minimum number density ν for entanglement is the critical overlap concentration ν^*, defined as

$$\nu^* = 1/L^3; \qquad \nu = \Phi/V_{\text{rod}} \tag{3}$$

Here Φ is the volume fraction of rods with volume V_{rod}. The effects of rod−rod interactions on D_r are commonly interpreted in terms of the overlap concentration ν/ν^*.[10,13] For low-shear viscosities of charged rods we recently found[11] that the effect of extensive double layers can be written as an effective increase of the rod length and rotational volume, using the scaling

$$\nu_{\text{eff}}^* = \frac{1}{L_{\text{eff}}^3} = \frac{1}{(L + \alpha\kappa^{-1})^3} \tag{4}$$

Here κ^{-1} is the Debye length, which is a measure for the thickness of the electric double layer, and α is a positive fit parameter. In the literature similar definitions of the effective particle dimensions are mentioned to take account of double layer interactions in the description of phase transitions and dynamic processes in dispersions of charged colloids.[17−19] The value of the fit parameter α depends on the particle shape, the surface charge density, and the ratio of κ^{-1} and the particle size. For the dispersions of (rigid) boehmite needles,[11] the fit parameter is $\alpha = 5$. Interestingly, solutions of the more flexible FD-virus[4] follow the same rescaling,[12] also with $\alpha = 5$. The low-shear viscosity η of Brownian rods is directly related to D_r, via[13]

$$\eta \approx \eta_0 + \frac{\nu kT}{30 D_{r,0}} + \frac{\nu kT}{10 D_r} \tag{5}$$

This suggests that a rescaling as in eq 4 also applies to the rotational diffusion. In section 4 we will test such a dynamic scaling for our relaxation data.

3. Experimental Section

Boehmite Dispersion. The particles (see Figure 1) were synthesized from aqueous aluminium alkoxide solutions, following Buining *et al.*[2] and have an average length $\langle L \rangle = 191$ nm (±26%) and an average diameter $\langle D \rangle = 8.5$ nm (±29%). The dispersions were dialyzed for 1 week in cellophane tubes against a continuous flow of deionized water, yielding a very viscous optically birefringent dispersion with pH = 5.5 and a particle volume fraction $\Phi = 0.37\%$. Conductivity measurements[11] indicate that the (monovalent) background electrolyte concentration c_b in the dialyzed dispersion is $c_b \approx 0.06\Phi$ mol/L. The ζ-potential of the boehmite rods was estimated from electrophoresis measurements (Coulter DELSA 440SX) to be 70 mV. Dynamic light scattering (DLS) from very dilute dispersions gave a translational diffusion coefficient $D_{t,0} = 2 \times 10^{-12}$ m^2/s.

Samples with lower rod concentrations and higher ionic strength were prepared by addition of respectively deionized water and a lithium chloride (LiCl p.a.) solution. The total electrolyte concentration, and thus the Debye length κ^{-1}, follows from the sum of the added [LiCl] and the (estimated) background electrolyte concentration c_b.

Rheo-optic Measurements. The dimensions of the shear cell (see Figure 2) satisfy the requirements for a narrow gap geometry and ensure that the shear rate reduces to 1% of the applied value within 30 ms after cessation of the flow. For each measurement 13 g of the freshly prepared sample was poured into the shear cell. A shear rate was applied for 10 s and then switched off, and the decay of the birefringence was sampled for 1000 points, evenly distributed over a time scale of 1−100 s. To increase the signal-to-noise ratio, 10−50 decay curves were averaged, and the averaged curve was normalized on the intensity at $t = 0$. For each sample the decay behavior was measured for four different shear rates: 621, 435, 186, and 62 s^{-1}. The sensitivity of the setup did not allow accurate measurement of the birefringence decay for volume fractions lower than 0.14%. Since the colloidal stability of boehmite rods is very sensitive to the ionic strength,[11,12] the LiCl concentration was limited to [LiCl] ≤ 1 mM. No flocculation was observed during the measurements, and the measured relaxation curves were reproducible. All measurements were carried out at 20 °C.

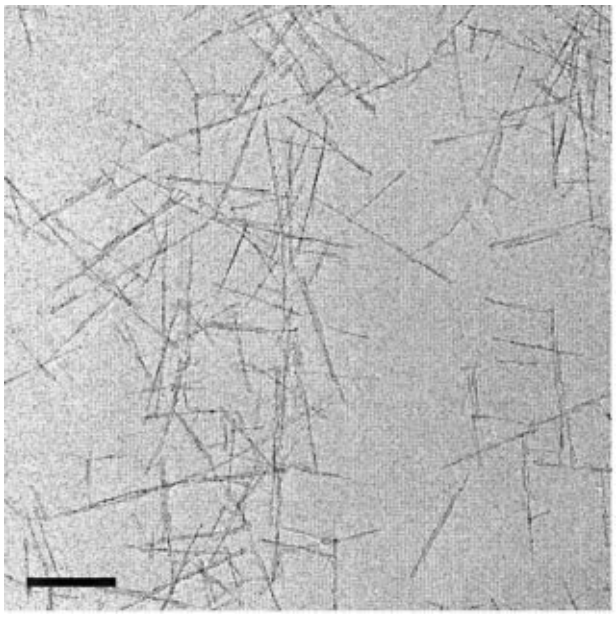

Figure 1. Transmission electron micrograph of the boehmite rods. The bar denotes 200 nm.

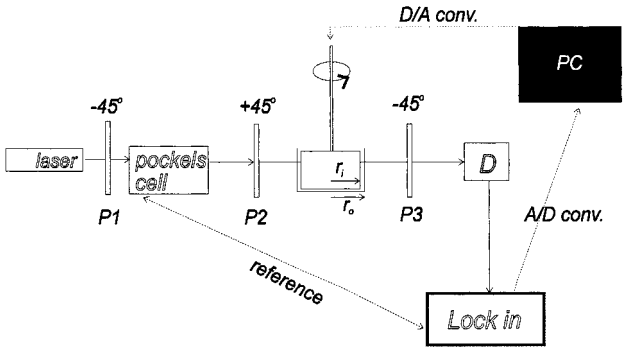

Figure 2. Schematic drawing of the rheo-optic setup. The incident laser beam ($l = 623.8$ nm) is modulated by a Pockels cell (EOD; 10 kHz). P1, P2, and P3 represent polarizers; D is the detector. The dimensions of the shear cell are $r_0 = 29.8$ mm and $r_i = 29.5$ mm. The shear field is applied by rotation of the inner cylinder of the Couette geometry (BK7-glass).

4. Results

Typical examples of decay curves are shown in Figure 3 (all other curves have a similar appearance). The "shoulder" in the curves between 0 and 100 ms is an artifact; the detector is not suitable for monitoring the fast changes in light intensity in this initial stage. For $t > 100$ ms only birefringence decay is observed. The graphs demonstrate the shear-rate dependence of birefringence relaxation; the rods show the fastest relaxation after application of the highest shear rate. This is probably due to the polydispersity in particle dimensions. For polydisperse rods, the birefringence decay of the dispersion

(17) Van Megen, W.; Snook, I. *Adv. Colloid Interface Sci.* **1984**, *21*, 119.
(18) Kralchevsky, P.; Denkov, N. *Chem. Phys. Lett.* **1995**, *240*, 386.
(19) Vroege, G. J.; Lekkerkerker, H. N. W. *Rep. Prog. Phys.* **1992**, *55*, 1241.

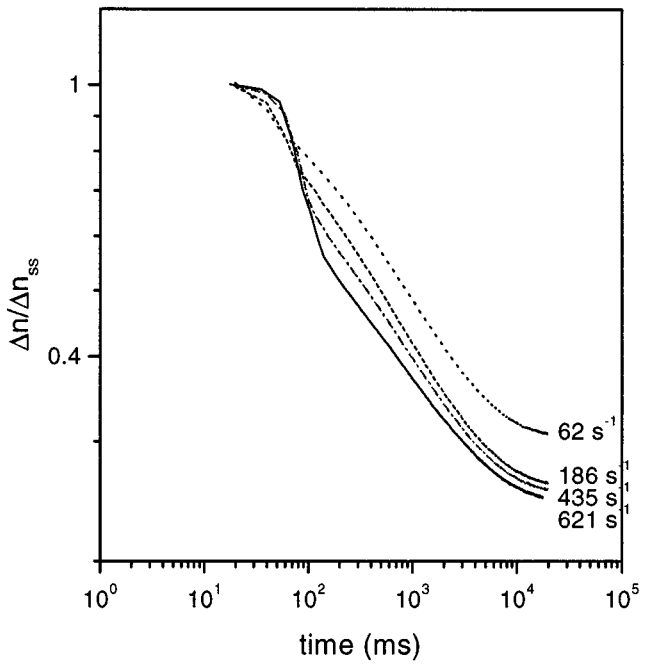

Figure 3. Typical birefringence decay curves for $\Phi = 0.28\%$ and [LiCl] = 0.201 mM, measured after cessation of shear for four different shear rates.

is a summation of exponential decays[20,21] of the form of eq 1. At low shear rates, only the longest rods in the sample will align, and the decay rate will be dominated by the relatively slow rotational diffusion of the longest rods. At high shear rates, also the short rods in the dispersion will align, and the average relaxation time of the aligned rods will decrease.[20−24] (Note that $Pe_{rot} \propto L^3$, eq 2.)

5. Discussion

In the following, we neglect the broad distribution of relaxation times, due to the polydispersity of the rods, and fit all curves by one single exponential, which represents the data fairly well for all systems. Thus the corresponding relaxation time τ_r characterizes the rotational diffusion of the whole sample and allows a qualitative comparison of the decay curves for different boehmite and electrolyte concentrations. Figure 4 shows the so-obtained rotational relaxation times for three different rod concentrations as a function of the electrolyte concentration c for $\dot{\gamma} = 62/s^{-1}$. The relaxation times are extremely long in comparison to free uncharged rods (for which eq 2 predicts $\tau_{r,0} = 8.3 \times 10^{-5}$ s). A second clear trend is that a small increase of ionic strength drastically reduces τ_r. This demonstrates that electric double layer interactions strongly affect the rotational dynamics of the boehmite rods. Using eq 4 we incorporate these interactions by a dynamic rescaling of the particle and electrolyte concentration, following:

$$\tau_r(\Phi,\kappa^{-1}) \rightarrow \tau_r(\nu/\nu_{eff}^*) \qquad (6)$$

For $\alpha = 5$ (the value found for low-shear viscosity data of boehmite dispersions and FD-virus solutions[11,4]), all

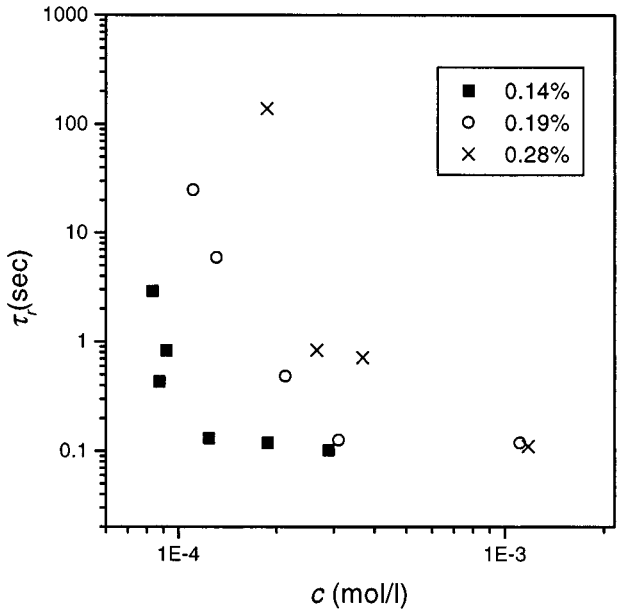

Figure 4. Rotational relaxation times τ_r for $\dot{\gamma} = 621$ s^{-1} (obtained from a single-exponential analysis of the birefringence curves) versus the total electrolyte concentration c, calculated from the known [LiCl], and the estimated background electrolyte concentration c_b.

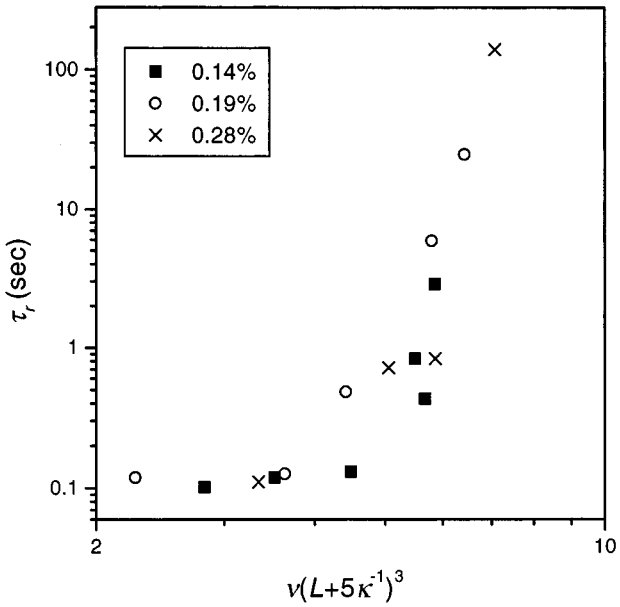

Figure 5. Rotational diffusion data from Figure 4 all fall onto one master-curve after rescaling the particle concentration as νL_{eff}^3, by defining $L_{eff} = L + 5\kappa^{-1}$. The relaxation time diverges for $\nu(L + \alpha\kappa^{-1})^3 \rightarrow (\nu/\nu_{eff}^*)_{gel} \approx 8$.

relaxation times from Figure 4 indeed form one master-curve (see Figure 5). We found exactly the same rescaling to apply for the relaxation behavior measured for lower initial shear rates.

For $\nu/\nu_{eff}^* < 4$, the characteristic relaxation time is only a weak function of the effective overlap concentration, but τ_r strongly increases in the range $\nu/\nu_{eff}^* = 4-8$. This steep increase of the relaxation time manifests the slowing down of the rotational dynamics on approach of the gel density Φ_{gel}. Above this threshold the Brownian diffusion is found to be completely arrested.[12] For dialyzed boehmite dispersions, the gel density determined from yield stress measurements[12] is $\Phi_{gel} \approx 0.3\%$. In the dialyzed boehmite dispersions, the electrolyte concentration is $c_b \approx 0.06\Phi$ mol/L (corresponding to $\kappa^{-1} \approx 23$ nm for

(20) Chow, A. W.; Fuller, G. G. *Macromolecules* **1985**, *18*, 786.
(21) Chow, A. W.; Fuller, G. G.; Wallace, D. G.; Madri, J. A. *Macromolecules* **1985**, *18*, 805.
(22) Marrucci, G.; Grizzuti, N. *J. Polym. Sci.,Polym. Lett. Ed.* **1983**, *21*, 83.
(23) Marrucci, G.; Grizzuti, N. *J. Non-Newtonian Fluid Mech.* **1984**, *14*, 13.
(24) Chow, A. W.; Fuller, G. G.; Wallace, D. G.; Madri, J. A. *Macromolecules* **1985**, *18*, 793.

$\Phi = 0.3\%$). We therefore expect a rescaled gel density of $\nu/\nu_{eff}^* \approx 8$. Inspection of Figure 5 shows that this value agrees remarkably well with the effective overlap concentration at which the rotational relaxation time diverges. This clearly demonstrates the direct relation between the rotational diffusion and low-shear rheology in rod dispersions; the rotational diffusion freezes at the same effective concentration at which a yield stress develops.

The data in Figure 5 suggest that extrapolation to $\nu = 0$ yields a value for $\tau_{r,0}$ which is much larger than the rotational relaxation time calculated for hard rods with the same dimensions ($\tau_{r,0} = 8.3 \times 10^{-5}$ s). A similar discrepancy is found for the translational diffusion coefficient $D_{t,0}$ measured with DLS on very dilute samples; its value is a factor 4 lower than that expected for a single hard rod. Also for low-shear rheology results at low density do not approach values for free hard rods.[11] This is very likely a consequence of the nonanalytic concentration dependence of the friction factor of colloids at extremely low particle density and ionic strength as discussed elsewhere.[11,25,26]

6. Conclusions

The rotational relaxation behavior of aqueous dispersions of charged boehmite needles ($\langle L \rangle / \langle D \rangle = 22.2$) was measured by analysis of the decay of optical birefringence after cessation of the shear flow. The rotational relaxation is strongly affected by electric double layer interactions, which can be taken into account by a rescaling of the particle and electrolyte concentration by redefinition of the rotational volume of the rods. The same rescaling applies for low-shear viscosity data of dispersions of boehmite and FD-virus.[11] The relaxation times clearly demonstrate a gradual freezing of the rotational dynamics on approach of the critical gel concentration, where a yield stress develops.

Acknowledgment. We thank Gerard Harder and Igno Dur for building the rheo-optic setup and Carel van der Werf for the installation of the equipment and assistance during the measurements.

LA9708593

(25) Yamakawa, J.; Matsuoka, H.; Kitano, H.; Ise, N. *J. Colloid Interface Sci.* **1990**, *134*, 92.

(26) Thies-Weesie, D. M. E.; Philipse, A. P.; Nägele, G.; Mandl, B.; Klein, R. *J. Colloid Interface Sci.* **1995**, *176*, 43.